Asian Journal of Chemistry; Vol. 27, No. 12 (2015), 4553-4562

ASIAN JOURNAL OF CHEMISTRY

http://dx.doi.org/10.14233/ajchem.2015.19228

Selective Transport of Fe(III) Using Polyeugenol as Functional Polymer with Ionic Imprinted Polymer Membrane Method

MUHAMMAD CHOLID DJUNAIDI[1,2,*], JUMINA[2], DWI SISWANTA[2] and MATHIAS ULBRICHT[3]

[1]Department of Chemistry, Faculty of Science and Mathematics, Diponegoro University, Semarang, Indonesia
[2]Department of Chemistry, Faculty of Mathematics and Natural Sciences, Gadjah Mada University, Yogyakarta, Indonesia
[3]Lehrstuhl für Technische Chemie II, Fakultät für Chemie, Universität Duisburg-Essen, 45117 Essen, Germany

*Corresponding author: Fax: +62 24 76480824; Tel: +62 24 76481452; E-mail: cholid_dj@undip.ac.id

Received: 7 April 2015; *Accepted*: 20 May 2015; *Published online*: 29 August 2015; AJC-17507

The synthesis of ionic imprinted polymer-Fe membrane using eugenol derivative (polyeugenol) had been done followed by its utilization study as functional polymer for selective transport of Fe(III). Eugenol was polymerized using BF_3-diethyl ether as catalyst. The polyeugenol was then bounded with an ion template [Fe(III)] followed by *in situ* crosslinking with polyethylene glycol diglycidyl ether and membrane base poly(vinyl alcohol) (PVA, M_r = 125,000) in 1-methyl-2-pyrrolidone. A membrane was obtained after casting at 25 m/s and soaking in NaCl solution for 2 days. The membrane soaked further in 0.1 M HCl solution to release Fe(III). The membrane was then analyzed using IR spectrometry, TGA-DTA, SEM and size selective test. Different optimizations steps were carried out for both the synthesis conditions and transport experiments. The selectivity of ionic imprinted polymer membrane for Fe(III) was studied using Cr(III), in separated systems with Cr(III) and Fe(III) in different solutions as well as using binary mixture solutions of the two metals. Experimental results indicate that the crosslinked ionic imprinted polymer membranes are more selective than non-imprinting polymers and as well as its constituents.

Keywords: Fe-ionic imprinted polymer membrane, Polyeugenol, Fe(III), Selectivity.

INTRODUCTION

Molecularly imprinted polymers (MIP) is considered an attractive synthetic materials due to its properties which mimics those of specific receptors in an antibody. In fact, molecularly imprinted polymers have gained considerable attention in the field of analytical chemistry during the last decade[1-4]. Molecularly imprinted polymers are stable, strong and resistant at a wide range of pH, solvent and temperature. In addition, this material can be easily and cheaply produced[5].

Today, heavy metal imprinted adsorbents used for the separation of selective heavy metals have attracted more attention, one of which is for the separation of Fe(III)[6-8]. The development of inexpensive adsorbents with high adsorption capacity had been the main goal of many studies. One interesting study is the use of biomaterials as adsorbent for heavy metal waste[9,10]. Biomaterials are very important because it is low-cost and biodegradable, as well as biocompatible. They can be prepared from a number of different agricultural wastes such as corn husk, bagase, rice husk, lignin, microbial biomass, chitosan[11,12] and eugenol. Eugenol is one of the native Indonesian natural products and has many purposes, including for the separation of metal ions. One example is the conversion of eugenol into polyeugeniloxy acetate used for the separation of heavy metal mixtures by solvent extraction method[13]; another example is its conversion into eugenoxy acetate for the separation of Cr(III) using bulk liquid membrane (BLM) method[14]. Eugenol polymer, polyeugenol, has been used as a bulk liquid membrane carrier with the order of Cr(III) >> Fe(III) > Ni(II) >> Zn > Cd (hard >> medium > soft)[15].

In the last decade, imprinting techniques had been used for the buildup of molecularly imprinting membranes (MIMs) able to selectively recognize target molecule(s) in a solution by simple adsorption or permeation through a membrane device[16]. Molecularly imprinted polymer membrane is a membrane containing molecule recognition sites and is usually prepared by molecular imprinting techniques. Benefits of molecularly imprinted polymer membranes include the availability of different preparation methods, highly flexible molecularly imprinted polymer membranes with high permeability as well as specific separation capacity for template and ligand. In addition, the use of molecularly imprinted polymer as affinity phase is useful for affinity-base separations as well as membrane sensors. Also, these membranes do not

need any additives and can be used at low temperature, thus reducing the cost for energy consumptions. Furthermore, compared to conventional application of imprinted polymer, molecularly imprinting membranes can be applied continuously due to the benefits of the membrane characteristics and molecule imprinting technology. In addition, molecularly imprinting membranes also showed improved selectivity while at the same time retaining the separation efficiency[16,17].

In the present study, molecularly imprinted polymer (ionic imprinted polymer) membranes had been prepared using polyeugenol as the functional polymer, poly(vinyl alcohol) as the membrane base as well as polyethylene glycol diglycidyl ether (PEGDE) as crosslinker, followed by the utilization of the membranes for Fe separation. Poly(vinyl alcohol) (PVA) was used because the material is chemically stable, hydrophilic, elastic, non-toxic, biodegradable and not carcinogenic[18]. Poly(vinyl alcohol)-base membranes prepared with KOH and PEGDE crosslinker are proved to have good mechanical strength and able to retain KOH permanently in the membrane. Here, PEGDE functioned not only as a crosslinking agent, but also as a plasticizer[19].

EXPERIMENTAL

All chemical reagents used are of analytical grade. Eugenol, boron trifluoride diethyl ether ($BF_3O(C_2H_5)_{2-}$), poly(vinyl alcohol) (PVA, M_r = 125000), polyethylene glycol diglycidyl ether (PEGDE), NaOH and HCl were purchased from Sigma-Aldrich, 1-methyl-2-pyrrolidone and Fe(III) nitrate nanohydrate were purchased from Fluka while demineralized water were from Milli Q. Finally the quantitative filter paper was purchased from Roth (20 s, größe 110 mm).

General procedure

Synthesis of polyeugenol: Eugenol (5.8 g) was placed in a 3-necked flask, then 0.25 mL of boron trifluoride diethyl ether [$BF_3O(C_2H_5)_2$] was added as catalyst. The addition was done 4 times every hour while stirring with magnetic stirrer at room temperature. The progress of the reaction can be characterized by a change of the solution into red. After the last addition of the catalyst, the polymerization was allowed to continue up to 12-16 h, after which 1 mL of methanol was added to stop the reaction. The gel produced was dissolved in chloroform and put into a separating funnel and then washed repeatedly with distilled water until neutral. The organic layer was transferred into a 50 mL Erlenmeyer flask and added with anhydrous Na_2SO_4. The liquid was then separated by decantation, after which the solvent was evaporated in a rotary evaporator at 40 °C. The residue obtained was further dried in the desiccator and was subsequently weighed and characterized using FT-IR.

Synthesis of ionic imprinted polymer-Fe(III) membrane: The imprinting process was started by stirring polyeugenol (0.5 g) with Fe(III) solution 50 ppm 10 mL for 24 h at pH 3. The product was filtered with a filter paper and subsequently air dried at room temperature.

Preparation of ionic imprinted polymer membrane: Polyeugnol (0.5 g) that has been crosslinked with Fe(III) was added with PVA (0.5 g) and dissolved in 6 mL of 1-methyl-2-pyrrolidone with an addition of NaOH as catalyst and PEGDE and subsequently heated at 100-110 °C for 4 h. The mixture was then allowed to cool overnight to form hydrogel. The hyrogel was then weighed and dissolved into 1-methyl-2-pyrrolidone and further heated until sufficient viscousity was reached and the gel ready to be cast. The casting was performed at 25 m/s on a piece of glass. The casting layer was then dried in an oven at 80 °C overnight. The membrane produced was then coagulated in 1.5 M NaCl solution for two days. After-wards, the membrane sheets was cut into smaller pieces and put on the ring of the diffusion cell and subsequently washed with demineralized water until neutral. Afterwards, Fe(III) was leached from the membranes using 0.1 M HCl solution for 24 h to produce ionic imprinted polymer-Fe(III) membranes.

Synthesis of non-imprinting polymer membranes: Non-imprinting polymer membranes were synthesized with the same method as that of molecularly imprinted polymer membrane excluding the imprinting process of Fe(III).

Fe(III) transport through membrane. The transport of Fe(III) through the membrane was measured using a diffusion cell. 50 mL Fe(III) solution (pH 3, 50 mg/L) and 50 mL of HCl 0.1 M were used as the feed phase and the stripping (recipient) phase, respectively. The process was carried out with stirring for 24 h.

Optimization of Fe(III)-ionic imprinted polymer-membranes performance. Performance optimization of Fe(III)-ionic imprinted polymer membrane was performed by varying feed phase pH, crosslinker concentration and membrane thickness as well as template.

Selectivity test for ionic imprinted polymer membranes: Selectivity test for ionic imprinted polymer membranes was done by comparing ionic imprinted polymer membranes to non-imprinting polymer membrane and was performed for separated solutions of Fe(III) and Cr(III) as well as a binary mixture solution of the two ions.

Detection method: The instruments used in this study are pH-meter, magnetic stirrer, separating funnel, glass wares and plastic wares, analytical balance (Mettler Toledo AB54-S), three-necked flask, casting machine (Erichsen), FTIR spectrophotometer (Jasco Miracle ATR), atomic absorption spectrophotometry (Shimadzu 8201PC), UV-visible (50 Probe), capillary flow porometer (PMIInc., NY, USA), contact angle goniometer (OCA 15 Plus, Dataphysics GmbH, Filderstadt, Germany), TOC-analyzer (Shimadzu) and a set of transport diffusion cell.

Contact angel measurement: The static contact angle with water was measured by Sessile drop method metode sessile drop using a contact angle goniometer (OCA 15 Plus, Dataphysics GmbH, Filderstadt, Germany) equipped with a video camera and image analysis software. 5 drops of 5 µL of water each was dropped on to the surface of the membrane to obtain the average contact angle of the membrane.

Total organic carbon (TOC) measurement: Diffusion measurement with total organic carbon was performed to determine the rate of diffusion through specific membrane (effective diffusion coefficient) and solute fractionation at this condition. The measurement was carried out using a diffusion cell comprising of two half-cells. The two half cells was filled with receiving solution (at the same time and to the same height

with 50 mL of water) and feed solution (10 g/L equimass mixture of dextran with average molecular weight of 15000 until 20000 (dextran 15) in 50 mL of water) and was stirred at the same rate. The diffusion of dextran through the membrane was monitored by measuring its concentration using total organic carbon in the two half cells for 24 h.

Pore size measurement: Pore size distribution was analyzed with gas/liquid displacement permporometry using capillary flow porometer by "dry up/wet up" method. The diameter of the membrane sample was 25 mm. The data from the first stage described the gas flow through the dry membrane. At the second stage, the instruments recorded the data for wetted membrane (wetting liquid: 1,1,2,3,3,3-hexafluoropropene ("Galwick", PMI Inc.), surface tension of 16 dyn cm^{-1}). The software would then calculate the pore size distribution based on the data for the dry and wet membranes. The pore diameter of the membrane is determined from the pore size distribution and the maximum pore size. The maximum TMP for the measurement of air flow was 5 bar.

Fe(III) analysis: The analysis of Fe(III) was mainly carried out using UV-visible spectroscopy with KSCN reagent at 458 nm. However, AAS was also used for Fe analysis in the binary solution mixture.

Cr(III) analysis: The analysis of Cr(III) was performed using UV-Visible spectroscopy at 420 nm. However, AAS was also used to analyze Cr(III) in the binary mixture solution.

RESULTS AND DISCUSSION

Contemporary formation of membrane structure and molecule recognizing sites were especially done by two methods, *in situ* crosslinking polymerization and alternative molecule imprinting. The first method allows the formation of crosslinking polymer induced by thermal energy or UV radiation which initiates the polymerization in a mixture solution or template, functional monomers, crosslinker in an appropriate solvent[16]. In this technique, functional monomer, crosslinker and template are mixed together in an appropriate solvent and was added with an initiator[20,21]. Using UV radiation or thermal energy, membranes will be formed, followed by the release of templates so that binding sites are formed in the membranes[22]. In the present study, membrane was obtained *in situ* by reacting polyeugenol (functional polymer), PVA, PEGDE (crosslinker) and NaOH (catalyst, initiator) in 1-methyl-2-pyrrolidone solvent at elevated temperature.

Synthesis of ionic imprinted polymer Fe membrane: As can be seen in Fig. 1, the synthesis of ionic imprinted polymer-Fe membrane comprises of four stages, starting with the polymerization of eugenol. Eugenol was polymerized using BF_3 diethyl ether as catalyst and resulted polyeugenol was characterized by FT-IR and NMR. To determine how many number (*n*) of eugenol molecules exist in the polyeugenol chain, gel permeation chromatography analysis was done. The characterization results of polyeugenol were reported in a different paper.

The polyeugenol was used for the synthesis ionic imprinted polymer membrane. This was done by uploading Fe(III) into the polyeugenol chain, followed by *in situ* crosslinking using PEGDE and PVA in 1-methyl-2-pyrrolidone solvent.

Variation of NaOH catalyst (initiator): The first stage in the synthesis of Fe-ionic imprinted polymer membrane was to optimize the concentration of NaOH that was used as the catalyst for crosslinking reaction between polyeugenol, PVA and PEGDE. The optimum concentration of the catalyst is important to determine, as too high concentration will result in the formation of precipitates and if too low concentration is used, crosslinking will not occur sufficiently. The experimental results are show in Table-1.

As presented in Table-1, using 1-methyl-2-pyrrolidone media, precipitate was formed when 0.4 M NaOH was used, the result of which is similar to that obtained from the formation of crosslinked polyeugenol-PEGDE in aqueous media. So, it is likely that crosslinking reaction between polyeugenol and PEGDE also occurred in 1-methyl-2-pyrrolidone media. Membrane 2 also produced precipitates as demonstrated by the tiny spots on the membrane surface, in contrast to the relatively clean surface of membrane 3. Therefore, membrane 3 was then used for the following processes as the NaOH concentration is still below the minimum concentration for the formation of precipitates resulted from crosslinking polymerization of eugenol-PEGDE observed in membrane 1 and 2. The darker of this membrane indicates that the concentration of the crosslinked polyeugenol still remain high. Meanwhile, low concentration of NaOH will cause the leaching of free polyeugenol during washing by NaCl and other steps, as was observed for membrane 4, 5 and 7.

The IR analysis of the membranes and the result can be seen in Fig. 2. Fig. 2 shows new and wide absorption band at 3300 cm^{-1}, which should indicate the crosslinking between

TABLE-1
NaOH VARIATION DURING MEMBRANE PREPARATION

Membrane	Crosslink poly-PEGDE		
	NaOH (M)	Total M NaOH in solution	Results
Membrane I	1 mL 2 M NaOH in 5 mL 1-methyl-2-pyrrolidone	0.4 M	Precipitates
Membrane II	1 mL 1 M NaOH in 5 mL 1-methyl-2-pyrrolidone	0.2 M	A number of spots can be observed at the membrane surface
Membrane III	1 mL 0.5 M NaOH in 5 mL 1-methyl-2-pyrrolidone	0.1 M	No precipitate on the membrane
Membrane IV	1 mL 0.25 M NaOH in 5 mL 1-methyl-2-pyrrolidone	0.05 M	Lighter of the membrane
Membrane V	1 mL 0.1 M NaOH in 5 mL 1-methyl-2-pyrrolidone	0.025	Lighter of the membrane
Membrane V I	-	1 mL water	Dilute solution, no membrane was formed.
Membrane V II	1 mL 0.1 M NaOH in 5 mL 1-methyl-2-pyrrolidone	1 mL water without PEGDE	Dilute solution, membrane was formed at the edge
PVA	1-Methyl-2-pyrrolidone	Without PEGDE	Very thin membrane, light
PVA-PEGDE	1-Methyl-2-pyrrolidone	With PEGDE	Very thin membrane, light

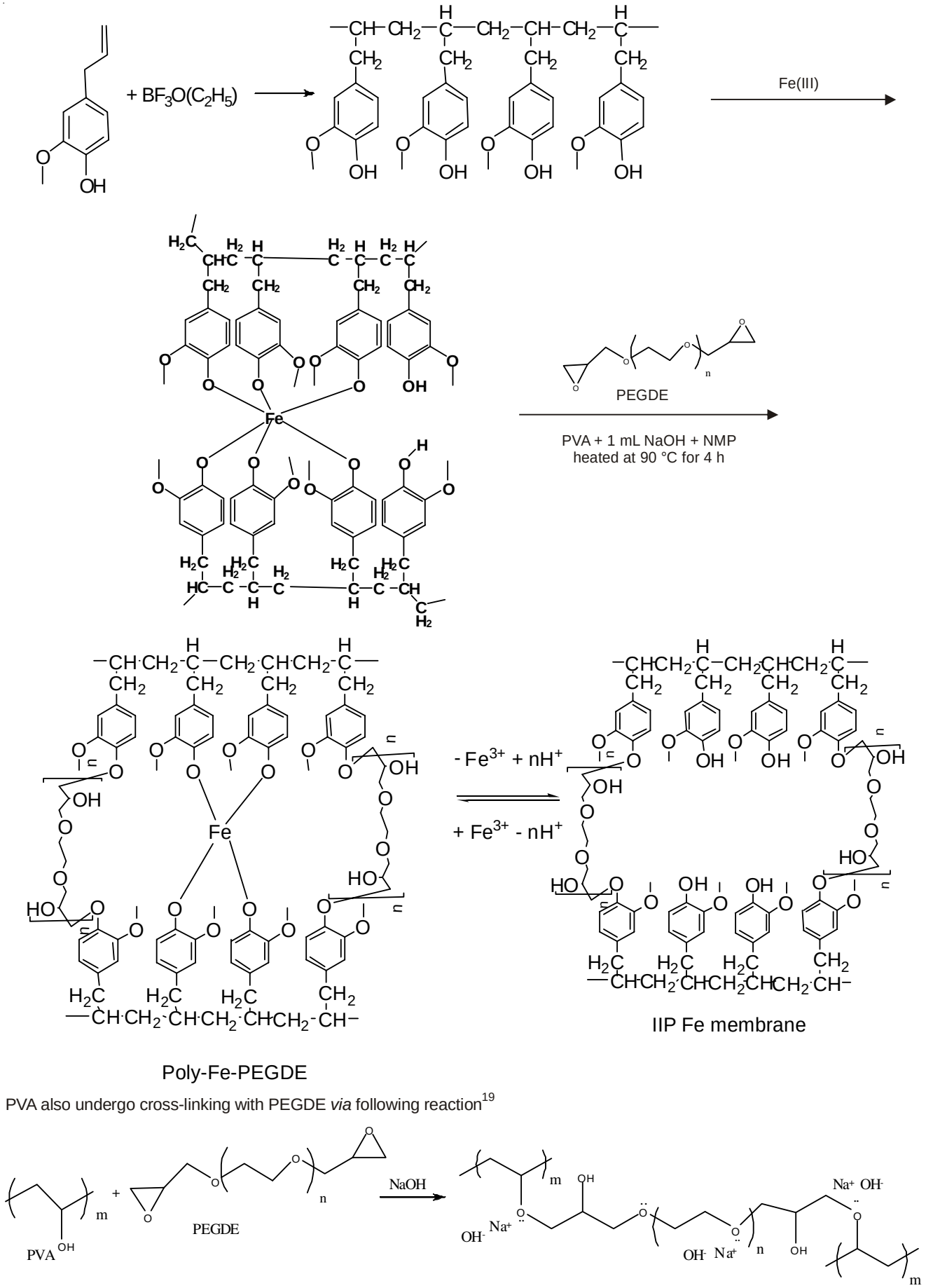

PVA also undergo cross-linking with PEGDE *via* following reaction[19]

Fig. 1. Synsthesis of ionic imprinted polymer-Fe membrane

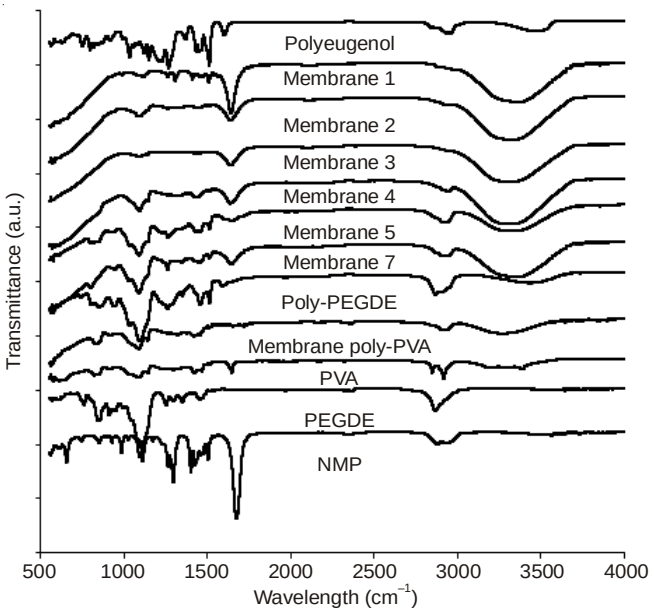

Fig. 2. Infrared spectra of the membranes for different NaOH concentrations

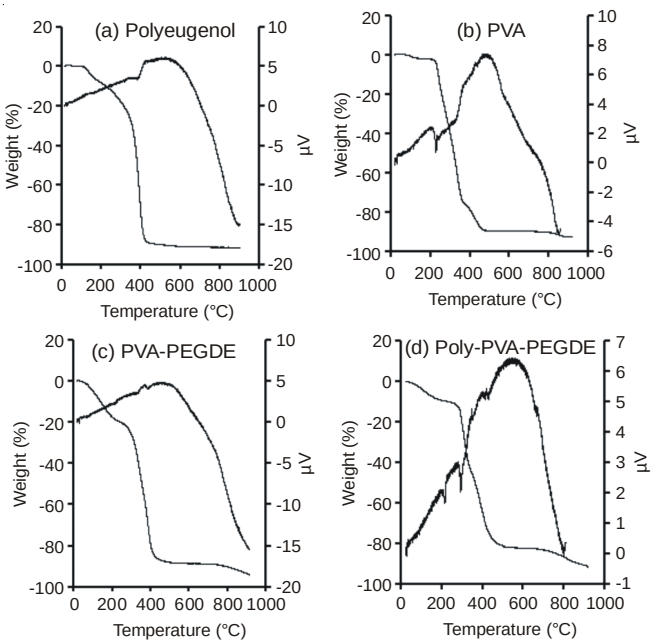

Fig. 3. TGA-DTA curves for different membranes

polyeugenol, PEGDE and PVA. Mean-while, the absorption band at 1100 cm^{-1} can be attributed to stretching vibration of -CO in EGDE. It can also be seen that the lower NaOH concentration, the absorption band of OH at 3300 cm^{-1} becomes weaker, but the band at 1100 cm^{-1} were stronger. This may be due to the smaller amount of crosslinking product and the higher content of free PEGDE in the membrane.

The TGA and DTA analysis were done to the crosslinking product as well as its components and the results can be seen in Fig. 3.

As can be seen at Fig. 3, the thermograph of PVA shows the weight loss of 9 % at 80 °C, which is caused by the evaporation of the adsorbed water molecules. The decomposition of the polymer started at 200 until 400 °C, with the total weight loss of 89 %. At this temperature range, PVA was degraded to produce water, ethanol, acetone, acetaldehyde and other compounds and the degradation is finalized at 600 °C[23]. The thermograph of PVA membrane/film only shows two steps, the evaporation of the moisture and the degradation of the polymer. This is different from that of both PVA crosslinked with PEGDE and PVA with polyeugenol, as more steps can be observed at higher temperature. It can also be seen that there is an increase of their chemical stabilities due to the crosslinking[19] and polyeugenol. The increase may be attributed to the presence of more intermolecular force which requires more energy to degrade[19].

From the DTA data in Fig. 3, it can also be seen that there is a weak endothermic peak at 226 ºC that can be ascribed to the melting point of PVA. The next endothermic peak that can be observed at 298 ºC and a wide exothermic peak at 521 ºC are due to the loss of water molecules and further degradation, which is in agreement with the TGA curves[23]. Fig. 3 also show that the degradation temperature of the crosslinking polymers is higher than that of PVA, where PVA-PEGDE and polyeugenol-PVA-PEGDE degraded at higher temperature than both polyeugenol and PVA. This is because the chemical structure became more stabile after crosslinking process.

Variation of hydrogel concentration: Membrane 3 was used then for the experiments to determine the optimum concentration of hydrogel. This was done by dissolving different amount of hydrogel in 1-methyl-2-pyrrolidone: 7 g of hydrogel in 1 mL 1-methyl-2-pyrrolidone, 4 g in 2 mL and 4 g in 3 mL, to produce membrane A, membrane B and membrane C, respectively. The casting thickness for each membranes are 500 μm for membrane A and 300 μm for both membrane B and C. The membranes were later used for the separation of Fe in the diffusion cell.

Experiments on the diffusion cell: The membranes that had been produced was later used for the transport of 50 mg/L Fe(III) in the feed phase using 0.1 M HCl in the recieving phase (stripping).

Experimental results indicate that there is a decrease of Fe(III) concentration in the feed phase, as demonstrated by the diminishing yellowish in the feed phase to become less after transport for 24 h. The data obtained after UV-visible analysis of the solutions are shown in Table-2.

TABLE-2
PERFORMANCE OF MEMBRANE A

Type of membrane A	Transport (%)			
	Feed phase 12 h	Stripping phase 12 h	Feed phase 24 h	Stripping phase 24 h
300 μ molecularly imprinted polymer	31.11	29.07	42.96	38.89
500 μ molecularly imprinted polymer	26.85	0	39.63	37.22
PVA 300 μ	29.43	28.49	39.62	38.30
PVA-PEGDE 300 μ	36.04	29.43	41.51	40.00

Membrane A: 7.25 g of hydrogel in 1 mL 1-methyl-2-pyrrolidone.

TABLE-3
PERFORMANCE OF MEMBRANE B AND C

Membrane	Transport (%)			
	Feed phase 12 h	Stripping phase 12 h	Feed phase 12 h	Stripping phase 12 h
4 g of hydrogel in 2 mL 1-methyl-2-pyrrolidone (B)	53.50	22.39	59.14	25.81
4 g of hydrogel in 3 mL 1-methyl-2-pyrrolidone (C)	54.03	29.30	65.32	30.65

Table-2 shows that for membrane A, when ionic imprinted polymer membranes are compared to its constituents, there is no significant difference in the transport percentage, indicating that the concentration of Fe(III) in the feed phase and the concentration of the hydrogel need to be decreased. Therefore, the following experiments used 4 g of hydrogel dissolved in 2 mL 1-methyl-2-pyrrolidone (membrane B) and 3 mL 1-methyl-2-pyrrolidone (membrane C) and Fe(III) concentration of 25 mg/L. The transport percentage based on UV-visible analysis results can be seen in Table-3.

Table-3 shows that membrane C performs better than membrane B for the transport of 25 mg/L Fe(III) from the feed phase, so that the membrane was then used for the following experiments.

The characterization results using SEM for each membranes are shown in Fig. 4, indicating that membrane A is more solid than the other membranes, especially when compared to the much more porous structure of membrane C. This was due to the high concentration as well as the thickness of membrane A (500 μm). After used for Fe(III) transport, the of the membranes seemed lighter as compared to the ones before (Fig. 4h), which might be the result of contact with HCl used as the stripping phase.

Optimization for membrane C (4 g hydrogel in 3 mL 1-methyl-2-pyrrolidone, with casting thickness of 300 μm)

Feed phase pH: The pH of the feed phase variation was done at pH 1, 2, 3, 4 and 5, while pH of the stripping phase was 1 (HCl 0.1 M). The % transport based on the analysis results can be seen in Fig. 5.

Fig. 5 showed that the feed phase optimum pH for Fe(III) transport was 3. This value is the same as the optimum pH for the adsorption of Fe(III) by ionic imprinted polymer-Fe adsorbent. The pH of the feed phase plays an important role in the speciation of Fe. At acidic condition, Fe(III) existed[24] as $[Fe(OH)]^{2+}$, $[Fe(OH)_2]^{+}$ and $[Fe_2(OH)_2]^{4+}$ and this ions will be difficult to be transported through the membranes with small pores. In addition, there is also a change in ionic charge of the hydroxyl as well as ether groups (C-O-C) of the membrane. At pH less than pKa, the functional groups will be protonated and thus decrease the transport percentage. Meanwhile, at pH higher than 5, Fe(III) will precipitate, so that the optimum pH of 3 was used for the following experiments.

Membrane thickness: The next optimization is for membrane thickness was optimized at 300, 500 and 700 μm during casting. The optimization experiments were carried out using 25 mg/L Fe(III) solutions and stirring time of 12 and 24 h. The analysis result is shown in Fig. 6.

It is clear from Fig. 6 that the membrane with 300 μm thickness exhibited better performance than the other two membranes for both 12 and 24 h stirring time. This might be because in the thicker the membrane, the active sides are overlapping with each other[25]. In addition, for thicker membranes, each Fe(III) ion must travel more distance during diffusion. From this result, the membrane with 300 μm thickness was used for the subsequent experiments.

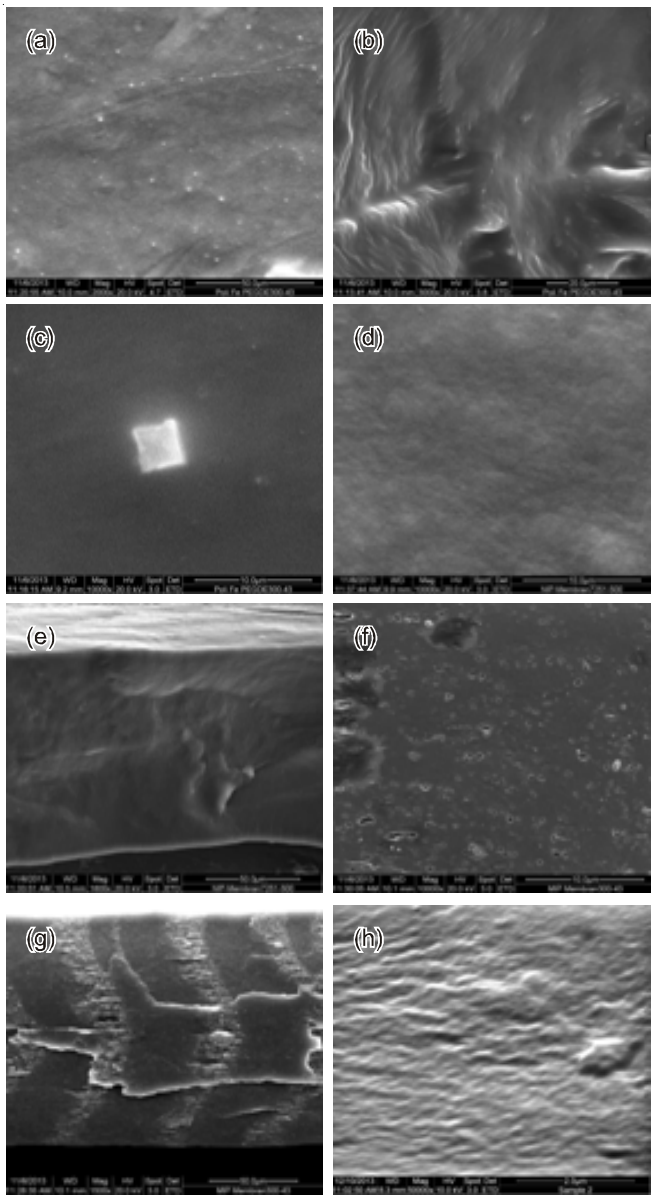

Fig. 4. SEM results of nembrane A and C; (a) Membrane poly-Fe-PEGDE C, front side, 2000x magnification; (b) Membrane poly-Fe-PEGDE C, cross section, 3000x magnification; (c) Membrane poly-Fe-PEGDE C, front side, 10000x magnification; (d) Membrane A front side flat, 10000x magnification; (e) Membrane A, cross section 1600x magnification; (f) Membrane C, front side flat 1000x magnification; (g) Membrane C, cross section, 1500x magnification; (h) Membrane C, fron side (flat), 500x magnification

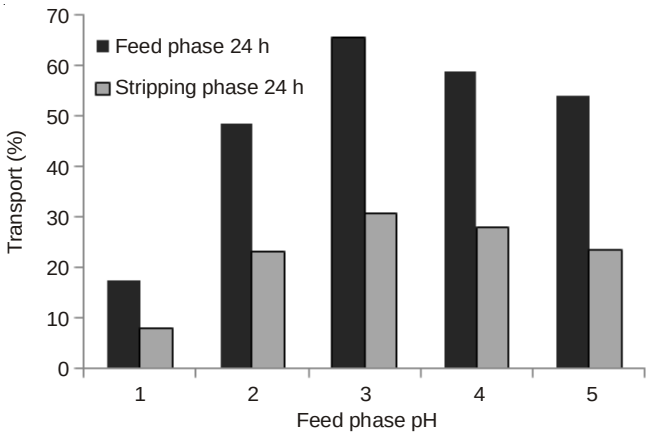

Fig. 5. Variation of feed pH for membrane C

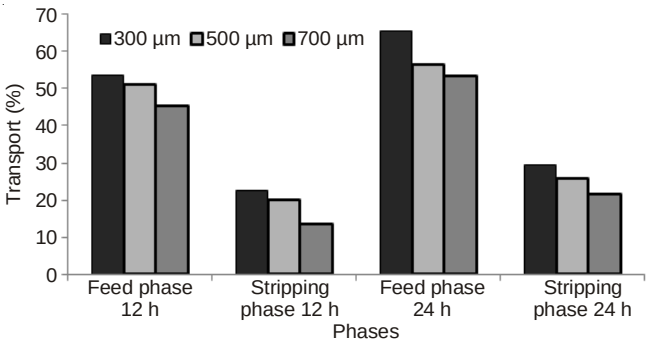

Fig. 6. Thickness variation for membrane C

Variation of crosslinker concentration: The optimization of crosslinking agent (PEGDE) were carried out through a series of experiments performed at the following conditions: feed phase pH 3, casting thickness of 300 µm using the membrane prepared from 4g hydrogel in 3 mL 1-methyl-2-pyrrolidone. For these experiments, the weight of PEGDE was varied at 0.38, 0.76, 1.52 and 2.28 g. The results were then analyzed with FITR spectra shown in Fig. 7.

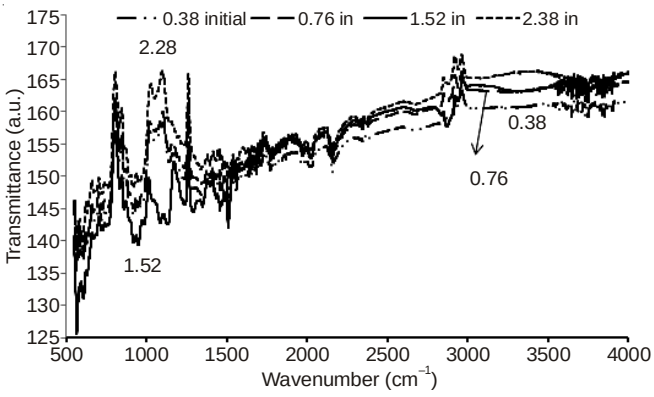

Fig. 7. Infrared spectra for different crosslinker weight

Fig. 7 showed that with the increase of PEGDE concentration, the absorption band for OH decreases while the band of glycidyl ether becomes sharper. It also shows that the sharpest absorption band of glycidyl ether was obtained when 1.52 g of PEGDE was used and thus this membrane is expected to be most selective compared to the others. Meanwhile, the result from TGA-DTA analysis is shown in Fig. 8.

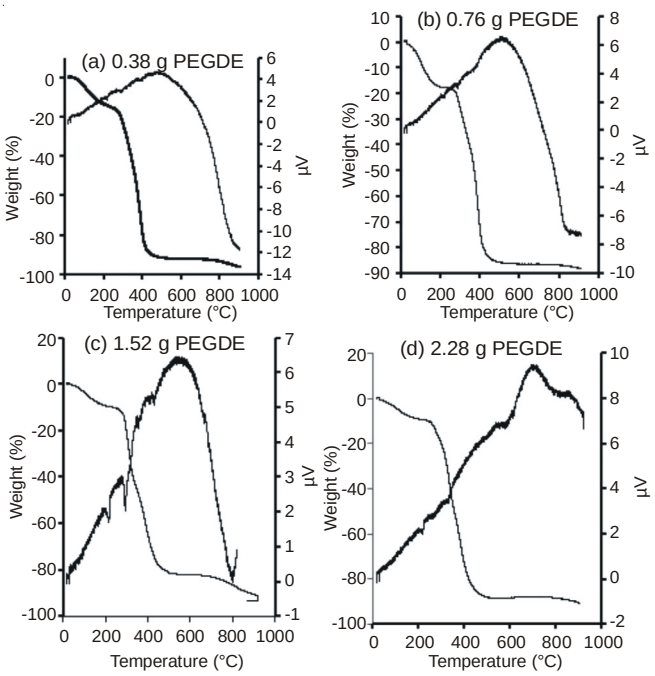

Fig. 8. TGA-DTA analysis for different membranes for different crosslinker concentration

It can be seen from Fig. 8 that at higher PEGDE concentration, the water related weight loss percentage at around 100 °C decreases. This might be due to the decrease of space in the membrane that can be filled with water molecules as these molecules were replaced by PEGDE. DTA analysis also agrees with the statement (Fig. 8). Fig. 8 also shows that the higher the PEGDE concentration, the higher the degradation temperatures, which should mean that the membranes are more chemically stable.

Based on contact angle analysis (Table-4), it can be seen that the contact angle increases with the increase of the crosslinker concentration, which can be attributed to the increase of the hydrophobicity of the membranes or the decrease of the hydrophilicity. This fact relates to the fact that poly(vinyl alcohol) is hydrophilic [19] and its amount decreases as the crosslinker increases.

TABLE-4
CONTACT ANGLE OF DIFFERENT MEMBRANE TYPES

Type of membrane	Contact angle
PVA	7.86
PVA-PEGDE	19.50
0.38	56.07
0.76	56.70
1.52	66.06
2.28	90.90

Meanwhile, the selectivity of the membranes were studied by using the membranes for the transport of Fe(III) and Cr(III), as both metals have similar charge density as well as ionic radius[7]. The experiments were carried out using separate solutions of 25 mg/L Fe(III) and 25 mg/L Cr(III) (pH 3) for the feed phase and 0.1M HCl (pH 1) for the stripping phase. The experimental results are displayed in Table-5.

TABLE-5
SELECTIVITY OF MEMBRANE C (4 g OF HYDROGEL IN 3 mL 1-METHYL-2-PYRROLIDONE)

Membrane	Transport (%) of [Cr] in the feed phase		Transport (%) of [Fe] of the feed phase		Selectivity	
	Cr 12 h	Cr 24 h	Fe 12 h	Fe 24 h	12 h	24 h
0.38	53.4	78.26	55.64	69.92	1.04	0.89
0.76	35	49.74	55.64	61.65	1.59	1.24
1.52	5.23	16.75	53.49	65.32	10.23	3.90
2.28	40.07	56.69	50.65	57.79	1.26	1.02
Non-imprinting polymers	43.97	43.31	30.83	37	0.70	0.85
PVA-PEGDE	36.18	48.43	33.3	37.95	0.92	0.78
PVA	56.98	64.39	47.17	57.98	0.83	0.90

Table-5 shows that all membranes after crosslinking have higher selectivity as compared to those of either each membrane components or non-imprinting polymer. The selectivity was obtained by dividing the transport percentage of Fe by that of Cr. In addition, from all membranes produced by crosslinking, the membrane with 1.52 g of PEGDE resulted in the highest selectivity, which may relate to the increasing sharpness of the glycidyl ether absorption band in IR spectrum (Fig. 7).

Proposed transport mechanism: There are two general mechanisms that usually used to analyze selective ion transport through imprinted membranes: (i) permeation facilitated by preferential affinity for the transport of the target molecule, so that the transport of competing ions will be prohibited and (ii) delayed permeation due to strong affinity toward the target molecules while the transport of other molecules is relatively faster until molecularly imprinted polymer sites is saturated with the target molecule[1-3].

From IR analysis of the membrane edge (not in contact with metal solutions) and middle membrane (in contact with metal solution), we proposed the transport mechanisms for both Cr(III) (Fig. 9) and Fe(III) (Fig. 10) as follows: (1) From Fig. 9, the proposed mechanism of Cr(III) transport involves the active OH and the glycidyl ether groups. This mechanism is supported by the decrease the absorption band intensities of both OH group (3000 cm^{-1}) and glycidyl ether (1100 cm^{-1}), which is apparent when the spectra of the active side and the non-active side of the membranes were compared. (2).This, however, is different from the proposed mechanism of Fe(III) transport which only involves the glycidyl ether functional groups, as marked by the decrease in the absorption band intensity for that group (Fig. 10).

Thus, from the analysis of Fe(III) transport, it can be concluded that the transport mechanism of Fe(III) in an *in situ* membrane is dominated by the first mechanism in which the template ion transport through permeation is driven by the active sites of glycidyl ether.

Size selectivity analysis using Dextran 15 pore size analysis using PMI: The diffusion of dextran through the membrane was monitored by measuring its concentration using total organic carbon in the two half cells for 24 h.

From Table-6, it can be seen that without acidification (C-W), which was done in order to leach the template ion, dextran molecules being released from the feed phase was relatively low. After acidification (C-AA) however, more dextran molecules were released from the feed phase. Thus, it can be concluded that the acidification was able to enlarge the pores. Table-6 also shows that the membrane without template ion Fe(III) (non-imprinting polymer C-AA) transported less dextran than ionic imprinted polymer membrane (C-AA), which means that the template ions also enlarged the pores after acidification. This conclusion is supported by pore size analysis using PMI, the result of which is shown in Table-7.

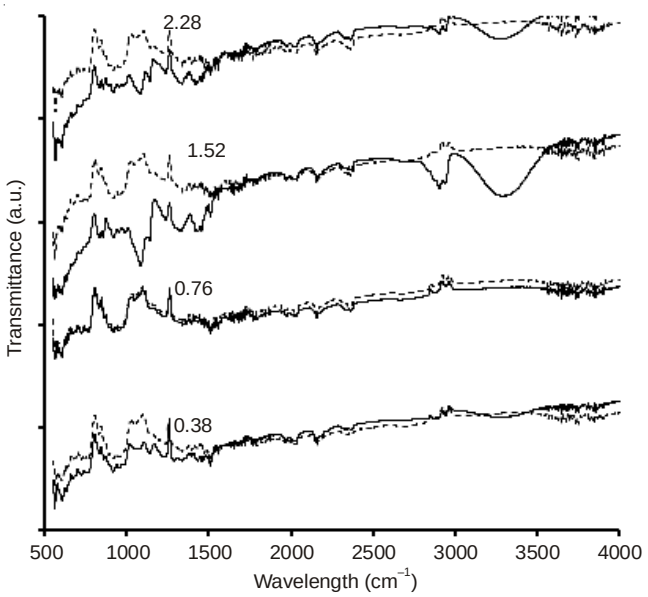

Fig. 9. Infrared spectra of membrane 0.38-2.28 after used for the transport of Cr(III) for membrane edge (—) and middle membrane (- - -)

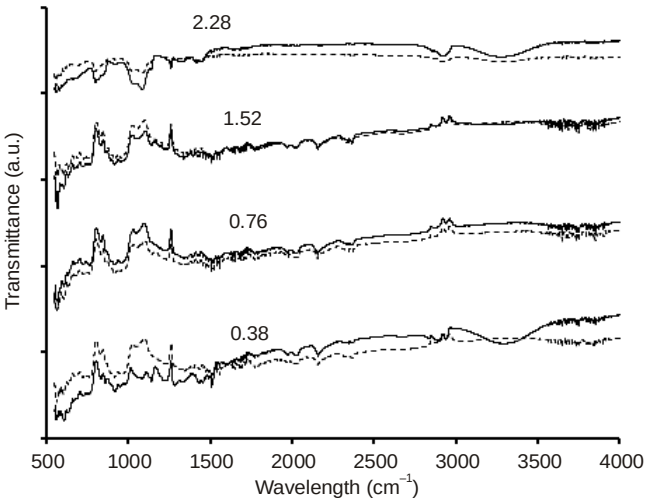

Fig. 10. Infrared spectra for membrane 0.38-2.28 after used for Fe(III) transport, for membrane edge (—) and middle membrane (- - -)

TABLE-6
SIZE SELECTIVITY ANALYSIS OF DIFFERENT MEMBRANES

Type of membrane	TOC measurement		Transport (%) of dextran 15
	Initial	24 h	
NIP C AA	2790	2684	3.8
C W	2790	2764	0.4
C AA	2689	2509	6.67

W = Water; NIP = Non-imprinting polymer; AA = After acid; W1 = Water, Without acid; TOC = Total organic carbon

TABLE-7
PORE SIZE ANALYSIS USING PMI

Type of membrane	Pore size distribution
C W	0 μ
C AA	0 μ
C AA 2x	0.17-0.3 μ

It can also be seen from Table-7 that after twice acidification (C-AA2x), the pore size became even bigger. This means that acidification is an important step during which the pores are enlarged so that they can be used for metal transport.

Variation of Fe(III) initial concentration in the feed phase: During metal transport process of metal ions, initial concentration of the metal ions plays an important role as the driving force for the mass transport. From Table-8, it can be seen the transport percentage of Fe(III) decreases with increasing Fe(III) concentration in the feed phase. This might be because at lower concentration, the concentration of the metal ions at the membrane is higher. As membrane has limited and fixed number of imprinted cavity, the number of metal ion that can be transported is also limited. At certain concentration, all imprinted cavities are filled with the metal ions. At this condition, the increase in metal ions concentration will not affect the transported metal ions and in fact can decrease the transport due to the decrease in metal ions activity in the solution[13].

TABLE-8
VARIATION OF Fe(III) INITIAL CONCENTRATION

[Fe(III)] (mg/L)	Transport (%)			
	Fp 12 h	Sp 12 h	Fp 24 h	Sp 24 h
25	53.49	30.1	65.32	30.64
50	45.99	27.81	58	29.95
100	41.66	34.76	47.33	39.93
200	25.12	14.76	35.44	33.79

Fp: Feed phase; Sp: Striping phase

Variation of Cr(III) concentration: To study the capacity of ionic imprinted polymer-Fe(III) membrane transporting Cr(III), the membrane was used for the transport of Cr(III). The concentrations varied at 25, 200 and 400 mg/L and the results are displayed in Table-9.

TABLE-9
VARIATION OF Cr(III) CONCENTRATION

[Cr(III)] (mg/L)	Transport (%) feed phase 12 h	Transport (%) feed phase 24 h
25	5.23	16.75
200	21.54	24.87
400	27.18	27.88

It can be seen from Table-9 that the transport percentage increases with increasing Cr(III) concentration, which might be because the transport mechanism does not involve any imprinted cavities and instead, the gradient concentration of metal ions between the feed phase and the stripping was the driving force for the mass transport in the membrane[1-3].

Variation of template ion concentration: To determine the effects of template ion concentration on the transport capacity of ionic imprinted polymer-Fe(III) membrane, a series of transport experiments were performed using membranes produced with following Fe(III) concentrations: 50, 100 and 200 mg/L. The template ion and its release from the membrane are two important factors in generating the imprinted cavities[16]. The experiments were carried out at pH 3 and 25 mg/L Fe(III) in the feed phase. The same experiments were also done separately for 50 mg/L Cr(III) solution using 0.1M HCl (pH 1) at the stripping phase. The experimental results are given in Table-10.

TABLE-10
TEMPLATE VARIATION

Type of membrane (mg/L)	Transport (%) in feed phase Fe(III) after 24 h	Transport (%) in feed phase Cr(III) after 24 h	Selectivity
50	65	16	4.0625
100	31	0	∞ (unlimited)
200	42.41	20.47	2.07

Table-10 suggested that membrane template ion 100 mg/L has the highest selectivity as compared to the other membranes. This is possibly due to smallest pores of the membranes were generated at this concentration, as supported by the result obtained from the diffusion test for dextran 15 solution, wherein the membrane with 100 mg/L template ions transported the smallest amount of Dextran (Table-11). These results were also supported by pore size measurement by PMI (Table-12).

TABLE-11
SIZE SELECTIVITY TEST USING DEXTRAN 15 USING TOC TEST

Types of membrane (mg/L)	Dextran released (%)
50	6.62
100	3.62
200	29.21

TABLE-12
PORE SIZE ANALYSIS FOR DIFFERENT TEMPLATES USING PMI

Type of membrane (mg/L)	Pore size distribution (μm)
50	0
100	0
200	0.13

Membrane selectivity test using binary mixture solution of Fe(III) and Cr(III): To study the selectivity of the membrane in a mixture, experiments using binary mixture solutions containing 25 mg/L Fe(III) and 25 mg/L Cr(III) at pH 3 as the feed phase and 0.1M HCl solution as the stripping phase. The solutions were then analyzed by AAS and the results are presented in Table-13.

TABLE-13
SELECTIVITY OF THE MEMBRANE FOR THE BINARY MIXTURE SOLUTION OF Fe(III) AND Cr(III)

Type of membrane (mg/L)	Fe % transport		Cr % transport		Selectivity	
	Fp 12 h	Fp 24 h	Sp 12 h	Sp 24 h	Fp 12 h	Fp 24 h
50	39.52	45.07	32.07	36.44	1.01	1.04
100	28.43	35.45	0	13.12	∞	2.70
200	42	44.6	31.15	31.85	1.35	0.89
Non-imprinting polymer	21.27	21.8	34.85	35.63	0.61	0.61

Fp: Feed phase; Sp: Stripping phase

As shown in Table-13, the selectivity of the membrane with 100 mg/L template ion performed better than non-imprinting polymer and other membranes, which is likely caused by the selective pores of the membrane towards Fe(III).

Conclusion

From this study, it can be concluded polyeugenol can be crosslinked *in situ* with PEGDE in 1-methyl-2-pyrrolidone solution. Ionic imprinted polymer-Fe membranes produced from the crosslinking showed high selectivity toward Fe(III). The membranes with highest performance for the transport of Fe(III) was obtained using 1.52 g of PEGDE and 100 mg/L Fe(III) as template ion. The selectivity mechanism of ionic imprinted polymer membranes is primarily due to transport facilitated by OH and glycidyl ether groups on the membranes.

ACKNOWLEDGEMENTS

One of the authors, Muhammad Cholid Djunaidi, express sincere gratitude to the members of the group of Prof. Mathias Ulbricht because this research was mostly performed during his stay at the University Duisburg-Essen, Essen, Germany and also to the Government of Republic of Indonesia for the Sandwich Program and Competitive Grant (Hibah Doctor).

REFERENCES

1. F. Trotta, M. Biasizzo and F. Caldera, *Membranes*, **2**, 440 (2012).
2. M. Ulbricht, *Polymer*, **47**, 2217 (2006).
3. M. Ulbricht, *J. Chromatogr. B Analyt. Technol. Biomed. Life Sci.*, **804**, 113 (2004).
4. J.O. Mahony, K. Nolan, M.R. Smyth and B. Mizaikoff, *Anal. Chim. Acta*, **534**, 31 (2005).
5. F.G. Tamayo, E. Turiel and A. Martín-Esteban, *J. Chromatogr. A*, **1152**, 32 (2007).
6. H.T. Fan and T. Sun, *Korean J. Chem. Eng.*, **29**, 798 (2012).
7. X. Chang, N. Jiang, H. Zheng, Q. He, Z. Hu, Y. Zhai and Y. Cui, *Talanta*, **71**, 38 (2007).
8. F. Xie, G. Liu, F. Wu, G. Guo and G. Li, *Chem. Eng.*, **183**, 372 (2012).
9. M. Sölener, S. Tunali, A.S. Özcan, A. Özcan and T. Gedikbey, *Desalination*, **223**, 308 (2008).
10. E. Guibal, *Sep. Purif. Technol.*, **38**, 43 (2004).
11. G.J. Copello, F. Varela, M. Vivot and L.E. Diaz, *Bioresour. Technol.*, **99**, 6538 (2008).
12. P. Miretzky and A.F. Cirelli, *J. Hazard. Mater.*, **167**, 10 (2009).
13. L. Harimu, S. Matsjeh, D. Siswanta and S.J. Santoso, *Indo J. Chem.*, **9**, 261 (2009).
14. M.C. Djunaidi, D.Trisna, *JSKA*, **13**, 2 (2010).
15. M.C. Djunaidi, R.A. Lusiana and P.J. Wibowa, *J. Alchemy*, **6**, 40 (2007).
16. C. Algieri, E. Drioli, L. Guzzo and L. Donato, *Sensors*, **14**, 13863 (2014).
17. N. Hilal, V. Kochkodan, L. Al-Khatib and G. Busca, *Surf. Interface Anal.*, **33**, 672 (2002).
18. B. Bolto, T. Tran, M. Hoang and Z. Xie, *Prog. Polym. Sci.*, **34**, 969 (2009).
19. G. Merle, S.S. Hosseiny, M. Wessling and K. Nijmeijer, *J. Membr. Sci.*, **409-410**, 191 (2012).
20. S.A. Piletsky, T.L. Panasyuk, E.V. Piletskaya, I.A. Nicholls and M. Ulbricht, *J. Membr. Sci.*, **157**, 263 (1999).
21. C. Geismann, A. Yaroshchuk and M. Ulbricht, *Langmuir*, **23**, 76 (2007).
22. C. Geismann and M. Ulbricht, *Macromol. Chem. Phys.*, **206**, 268 (2005).
23. X.-F. Lei and J.-X. Ma, *J. Braz. Chem. Soc.*, **21**, 209 (2010).
24. F.C. Baes and R.E. dan Mesmer, The Hydrolysis of Cations, John Wiley, New York (1976).
25. A.A. Kiswandono, D. Siswanta, N.H. Aprilita and S. Santosa, *Indo. J. Chem.*, **12**, 105 (2012).